

Nearby low-luminosity GRBs as the sources of ultra-high energy cosmic rays revisited

Ruo-Yu Liu^{1,2}, Xiang-Yu Wang^{1,2*}, and Zi-Gao Dai^{1,2}

¹ Department of Astronomy, Nanjing University, Nanjing, 210093, China

² Key laboratory of Modern Astronomy and Astrophysics (Nanjing University), Ministry of Education, Nanjing 210093, China

ABSTRACT

Low-luminosity gamma-ray bursts (GRBs) with luminosity $\lesssim 10^{49} \text{ ergs}^{-1}$ probably constitute a distinct population from the classic high-luminosity GRBs. They are the most luminous objects detected so far within ~ 100 Mpc, the horizon distance of ultra-high energy cosmic rays (UHECRs), so they are considered to be candidate sources of UHECRs. It was recently argued that the energy production rate in UHECRs is much larger than that in gamma-ray photons of long GRBs measured by the *Fermi* satellite, which, if true, would challenge the view that GRBs can be the sources of UHECRs. We here suggest that many of the low-luminosity GRBs, due to their low luminosity, can not trigger the current GRB detectors and hence their contribution to the local gamma-ray energy production rate is missing. We find that the real local energy production rate by low-luminosity GRBs, taking into account the missing part, which constitutes a dominant fraction of the total amount, could be sufficient to account for the flux of UHECRs. Due to the low-luminosity, only intermediate-mass or heavy nuclei can be accelerated to $\sim 10^{20}$ eV. We discuss the acceleration and survival of these UHE nuclei in low-luminosity GRBs, especially in those missing low-luminosity GRBs. At last, the accompanying diffuse neutrino flux from the whole low-luminosity GRB population is calculated.

Key words: cosmic rays – gamma ray: bursts

1 INTRODUCTION

Although the transition energy from galactic to extragalactic origin in high-energy cosmic ray spectrum remains inconclusive, there is a general consensus that cosmic rays with energy above the Greisen-Zatsepin-Kuzmin (GZK) energy of $E \gtrsim E_{\text{GZK}} = 4 \times 10^{19}$ eV, are of extragalactic origins. These UHE particles, whether they are protons or heavy nuclei, are attenuated when they are propagating in the intergalactic space. UHE protons with energies above the GZK cutoff undergo photopion interactions with cosmic microwave background (CMB) photons with an attenuation length of ~ 100 Mpc. Coincidentally, heavy nuclei with energy $\gtrsim 50 \text{ EeV}$ will suffer from a strong photo-disintegration attenuation due to interactions with CMB and cosmic infrared background (CIB), with an attenuation length $\lesssim 100$ Mpc. As a result, sources producing UHECRs above $E \gtrsim E_{\text{GZK}}$ must be within ~ 100 Mpc. Within this so-called GZK horizon distance, there are few sources that are powerful enough to be able to accelerate particles to energies $\sim 10^{20}$ eV. The candidates include local active galactic nucleus (AGN) jets (e.g. Biermann & Strittmatter

1987; Berezhinsky, Gazizov, & Grigorieva 2006), local GRBs (Waxman 1995, 2004; Vietri 1995; Wick, Dermer, & Atoyan 2004; Dermer & Atoyan 2006; Murase & Nagataki 2006; Murase et al. 2006), and semi-relativistic hypernovae remnants (Wang et al. 2007a). To accelerate UHECRs, the luminosity of the accelerators must satisfy the requirement $L \gtrsim 1.5 \times 10^{42} \text{ ergs}^{-1} (\Gamma^2/\beta)(E/10^{20} \text{ eV})^2 (Z/26)^{-2}$, where Γ and β are the bulk Lorentz factor and the velocity of the shock respectively, Z is the nuclear charge number of accelerated particles (Waxman 2005; Farrar & Gruzinov 2009; Lemoine & Waxman 2009). The brightest sources within this distance are nearby low-luminosity GRBs (LLGRBs) associated with hypernovae, e.g. GRB980425 with peak luminosity $L \sim 5 \times 10^{46} \text{ ergs}^{-1}$ at a distance 40 Mpc (associated with SN1998bw) and GRB060218 with $L \sim 5 \times 10^{46} \text{ ergs}^{-1}$ at distance 140 Mpc (associated with SN2006aj). They are much dimmer than their high-luminosity brothers, which are, however, detected at high redshifts. As a special subclass of GRBs, these nearby GRBs/hypernovae have been proposed to be candidate sources of UHECRs (Murase & Nagataki 2006; Wang et al. 2007a). Wang et al. (2007b) suggest that GRB060218-like LLGRBs may arise from the breakout of semi-relativistic ($\Gamma \sim 2$), radiation-dominated shocks from the progenitor stars of

* E-mail: xywang@nju.edu.cn

hypernovae or dense stellar wind surrounding the progenitor stars. In this scenario, UHECRs can be accelerated at the forward shock formed when the semi-relativistic ejecta is expanding in the stellar wind. In the scenario proposed by Murase & Nagataki (2006), LLGRBs are thought to arise from internal shocks in relativistic outflow with $\Gamma \sim 10$, similar to the case of high-luminosity GRBs, and UHECRs are accelerated by the same internal shocks.

GRBs are discovered preferentially at high redshifts ($z \gtrsim 0.5$) with an isotropic-equivalent energy of $E_\gamma \gtrsim 10^{51-54}$ erg, released in a few tenths of seconds to a few tens of seconds. So far only several nearby GRBs within ~ 200 Mpc are detected. GRB 980425, associated with hypernova 1998bw, is the first-found peculiar burst detected by *BeppoSAX* and BATSE at a distance of 38 Mpc, with an isotropic-equivalent total emitted energy of only $\sim 9.3 \times 10^{47}$ erg in 1-10000keV band¹ and a duration of ~ 35 s (Galama et al. 1998; Kulkarni et al. 1998; Pian et al. 1999; Kaneko et al. 2007). GRB 031203, associated with hypernova 2003lw, was detected by *INTEGRAL* at $z = 0.105$ with an isotropic-equivalent bolometric energy of $\sim 1.7 \times 10^{50}$ erg and a duration of ~ 37 s (Malesani et al. 2004; Prochaska et al. 2004; Kaneko et al. 2007). GRB 060218, associated with hypernova 2006aj, was detected by *Swift* at a distance of 140 Mpc, with an isotropic-equivalent energy of $\sim 4.3 \times 10^{49}$ erg and a duration of ~ 2100 s (Campana et al. 2006; Mirabal et al. 2006; Pian et al. 2006; Kaneko et al. 2007). GRB100316D, associated with SN 2010bh, was detected by *Swift* at distance of 260 Mpc, with an isotropic-equivalent bolometric energy larger than 5.9×10^{49} erg and a duration about 1300s (Chornock et al. 2010; Starling et al. 2011). All these nearby GRBs have low luminosity and are therefore named low-luminosity GRBs (LLGRBs). Due to their proximity, the inferred intrinsic rate of LLGRBs is, however, much higher (Soderberg et al. 2006; Liang et al. 2007; Guetta & Della Valle 2007; Dai 2009) than high-luminosity GRBs (HLGRBs). By checking whether the event rate of LLGRBs is consistent with a natural extrapolation of HL GRBs to low luminosity in a coherent luminosity function (LF), it is found that LLGRBs likely form an intrinsically distinct population from HLGRBs (e.g. Liang et al. 2007; Guetta & Della Valle 2007; Dai 2009; Virgili, Liang, & Zhang 2009).

Recently, Eichler et al. (2010) find that the energy production rate in UHECRs above 4EeV is about $10^{2.5}$ times larger than that contained in gamma-rays recorded by Fermi from long GRBs. This appears to be an overestimate, as later calculation by Waxman (2010) shown that the energy production rates in gamma-ray photons of GRBs and extragalactic UHECRs are comparable if some factors are taken into account carefully. The discrepancy may be caused by a combination of three factors: 1) Eichler et al. (2010) assumed that the extra-galactic CR production rate is about 10 times larger than the UHECR production rate, arguing that the generation spectrum of the extra-galactic cosmic rays extends to energy smaller than 10^{18} eV (note the spectrum is $dn/d\varepsilon \propto \varepsilon^{-2.7}$), while the estimate by Waxman (2010) only includes UHECRs above 10^{19} eV; 2) they assumed different transition energy at which the flux of extra-galactic cosmic rays dominates over the flux of the Galactic cosmic rays. Eichler et al. (2010) assumed that extra-galactic cosmic ray flux dominates over the Galactic component at 4×10^{18} eV, while Waxman (2010) assumed that it is dominated above 10^{19} eV;

3) Waxman (2010) also pointed out that the gamma-ray production rate in Eichler et al. (2010) is under-estimated, arguing that many distant/faint bursts are missed by Fermi/GBM.

Motivated by this problem, we revisit the scenario of LLGRBs as the accelerators of UHECRs and study whether the energy budget in LLGRBs is sufficient. Because of the low luminosity of LLGRBs, a lot of them may not trigger the detector and have therefore eluded detection. However, these dim GRBs may be still powerful enough to accelerate UHECRs.

For these LLGRBs, only inter-mediate mass or heavy nuclei can be accelerated to energies $\sim 10^{20}$ eV. The composition of the observed ultra high energy cosmic rays remains disputed. Recent observations of the Pierre Auger Observatory (PAO) show a transition in the maximum shower elongations $\langle X_{\max} \rangle$ and in their fluctuations $\text{RMS}(X_{\max})$ between 5EeV and 10EeV (Abraham et al. 2010). These transitions are interpreted as reflecting a transition in the composition of UHECRs in this energy range from protons to intermediate mass nuclei. However, this claim depends on the poorly-understood hadronic interaction models at such high energies. There is a long-lasting tension between the spatial UHECR-Active Galactic Nuclei (AGNs) correlation suggesting protons, and Auger results of X_{\max} and $\langle X_{\max} \rangle$ suggesting a significant heavy element component for UHECR in the same energy range. Recent update results of PAO show that the significance of the correlation between UHECRs and nearby extragalactic matter is decreased (The Pierre AUGER Collaboration et al. 2010), which relieves this tension to some extent and allow the possibility of a heavier composition.

To show whether LLGRBs can be sources of UHE nuclei, one also needs to know the survival probability of UHE intermediate-mass or heavy nuclei in the sources and the origin of these nuclei. For the semi-relativistic hypernova scenario, Wang, Razzaque, & Mészáros (2008) have shown that intermediate-mass or heavy nuclei can easily survive in the hypernova remnant shocks as the shock size is typically very large. In this scenario, one would also expect a natural origin of intermediate-mass to heavy nuclei since hypernova remnants are expanding in the stellar wind of the progenitor star of hypernovae, in which intermediate mass nuclei, such as O and C, are enriched. For the internal shock scenario, Murase et al. (2008) discussed the survival probability of heavy nuclei in LLGRBs for a certain set of parameter values of the luminosity, shock bulk Lorentz factor and peak energy of the photon spectrum. However, these parameters may vary for different LLGRBs and there are some inherent correlations among them. We will study their effects on the survival of UHECR nuclei, especially in those dim LLGRBs that do not trigger the detector. If these non-triggered LLGRBs are also able to inject UHECRs into the universe, they will contribute to the energy production rate in UHECRs, but not to that in gamma-ray photons recorded by detectors.

The paper is organized as follows. In §2, we estimate the ratio of gamma-ray energy production rates between the missing local LLGRBs and the observable local LLGRBs, as well as the local gamma-ray and UHECRs energy production rates for two luminosity functions. We discuss the acceleration and survival process of UHE heavy nuclei in sources, especially in those LLGRBs that may be missed by the detector in §3. In §4, we calculate the accompanying neutrino flux, contributed by all LLGRBs in the whole luminosity range. We give our conclusion in §5. Throughout the

¹ hereafter, unless otherwise specified, the "energy" or "luminosity" refers to this isotropic-equivalent bolometric (in 1-10000keV band) one

paper, unless otherwise specified, we use eV as the unit of particle energy and use c.g.s units for other quantities and denote by Q_x the value of the quantity Q in units of 10^x .

2 THE LOCAL ENERGY PRODUCTION RATE BY LLGRBS

To know the local energy production rate by LLGRBs, one needs to know the luminosity function (LF) of LLGRBs and then sum the contributions by all LLGRBs over the whole range of luminosity. Considering that LLGRBs probably form a distinct population from HLGRBs, here we adopt the LFs of the broken power-law form given by Liang et al. (2007) and Dai (2009). The first one has a form (Liang et al. 2007)

$$\frac{dN}{dL} = \rho_0 \Phi_0 \left[\left(\frac{L}{L_b} \right)^{\alpha_1} + \left(\frac{L}{L_b} \right)^{\alpha_2} \right]^{-1} \quad (1)$$

where ρ_0 is the local event rate of LLGRBs inferred from the observed ones, and Φ_0 is a normalization constant to guarantee the integral over the luminosity function being equal to the local event rate ρ_0 . In this luminosity function, the total local LLGRB rate is insensitive to the minimum luminosity, but fixed by the break luminosity L_b . We take the best fit values for these parameters from Liang et al. (2007) in our following calculation, i.e. $\rho_0 = 325 \text{ Gpc}^{-3} \text{ yr}^{-1}$, $L_b = 10^{47} \text{ ergs}^{-1}$, $\alpha_1 = 0$, and $\alpha_2 = 3.5$.

Another LF for LLGRBs is suggested as (e.g. Dai 2009)

$$\frac{dN}{dL} = \rho_0 \left[\left(\frac{L}{L_b} \right)^{-\alpha_1} + \left(\frac{L}{L_b} \right)^{-\alpha_2} \right], \quad (2)$$

which describes HL and LLGRBs together in one form with different power-law index, joined at the break energy. Here we take $\rho_0 = 1.7 \text{ Gpc}^{-3} \text{ yr}^{-1}$, $L_b = 5 \times 10^{48} \text{ ergs}^{-1}$, $\alpha_1 = 2.3$ and $\alpha_2 = 1.27$, which are suggested by Dai (2009) as the best fit values. In this LF, the local event rate of LLGRBs is sensitive to the minimum luminosity. The total event rate of LLGRBs is hard to know since the majority of LLGRBs at the low-luminosity end could be missed from detection. In principle, the total event rate of LLGRBs must be lower than the total rate of type Ib/c supernovae, $\sim 2 \times 10^4 \text{ Gpc}^{-3} \text{ yr}^{-1}$ (e.g. Cappellaro, Evans, & Turatto 1999; Dahlen et al. 2004). The fraction of Ib/c supernovae (SNe) which have relativistic outflows is a somewhat uncertain number. Radio observations of a large sample of Ib/c SNe suggest that less than 10% of Ib/c SNe are associated with GRBs (Soderberg et al. 2006). We assume two representative values for the ratio of the local event rate of LLGRBs to that of Type Ib/c SNe, i.e. $\xi = 1\%$ and $\xi = 10\%$ in the following calculation. With these ratios, one can get the minimum luminosity L_{\min} for the LF, as shown in Table 1.

With the LFs given above, we can now calculate the local gamma-ray energy production rates by LLGRBs

$$\dot{W}_\gamma(0) = \int_{L_{\min}}^{L_{\max}} E_\gamma(L) \frac{dN}{dL} dL, \quad (3)$$

where $E_\gamma(L)$ is the isotropic equivalent gamma-ray energy output for LLGRBs with luminosity L . The relation between E_γ and L is unknown for LLGRBs due to the small sample detected so far. We assume $E_\gamma \propto L^k$, where we take a wide range for k , i.e. $k \in (0, 1)$. We take the isotropic gamma-ray energy in GRB 060218 and GRB 100316D as a reference value, i.e. $E_\gamma =$

$LT_{90} = 10^{50} \text{ erg}$, where $L = 10^{47} \text{ ergs}^{-1}$ and $T_{90} = 1000 \text{ s}$. We set the upper limit of integral at $L_{\max} = 10^{49} \text{ ergs}^{-1}$. For the LF in Liang et al. (2007) (hereafter, LFL), there is no constraint on L_{\min} since the total local LLGRB rate is insensitive to the minimum luminosity. Setting L_{\min} to $5 \times 10^{45} \text{ ergs}^{-1}$, which is sufficiently low to contain all the LLGRBs that have been observed to date, we have $\dot{W}_\gamma(0) \simeq 3.25 \times 10^{43} \text{ ergMpc}^{-3} \text{ yr}^{-1}$ for $k=0$ and $2.72 \times 10^{43} \text{ ergMpc}^{-3} \text{ yr}^{-1}$ for $k=1$. The results are comparable for the case of $L_{\min} = 5 \times 10^{46} \text{ ergs}^{-1}$, as shown in Table. 1. On the other hand, for the LF of Dai (2009) (hereafter, LFD), depending on the minimum luminosity L_{\min} of the luminosity function, $\dot{W}_\gamma(0)$ is in the range of $(2 - 20) \times 10^{43} \text{ ergMpc}^{-3} \text{ yr}^{-1}$ for $k=0$ and $(8.42 - 14.9) \times 10^{43} \text{ ergMpc}^{-3} \text{ yr}^{-1}$ for $k=1$. The results of $\dot{W}_\gamma(0)$ are given in Table 1. These values are larger than that obtained in Eichler et al. (2010) by one to two orders of magnitude. Furthermore, the fact that the energy production rate in the $k=1$ case is less than that in the $k=0$ case in the lower L_{\min} case indicates that most gamma-ray energy production rate is contributed by LLGRBs with relatively low luminosities (e.g. $L < 10^{47} \text{ ergs}^{-1}$), which may be difficult to be detected by current GRB detectors.

We now discuss how much the missing LLGRBs contribute to the local energy production rate. To be detected by *Fermi*/GBM, a GRB located at a distance D requires to be brighter than a limit luminosity $L_{\text{lim}} = 4\pi D^2 S_{\text{GBM}}/B(e_1, e_2)$, where $S_{\text{GBM}} = 1.75 \times 10^{-8} \text{ ergcm}^{-2} \text{ s}^{-1}$ is the sensitivity of *Fermi*/GBM in its burst trigger band (50-300keV, von Kienlin et al. 2004; Band 2008; Imerito et al. 2008) and $B(e_1, e_2)$ is the energy fraction in the detector frequency window. $B(e_1, e_2)$ is given by (Bloom, Frail, & Sari 2001; Imerito et al. 2008)

$$B(e_1, e_2) = \frac{\int_{e_2}^{e_1} \varepsilon n(\varepsilon) d\varepsilon}{\int_{E_2}^{E_1} \varepsilon n(\varepsilon) d\varepsilon} \quad (4)$$

where e_1 and e_2 are the upper and lower threshold energy of the detector, while E_1 and E_2 are upper and lower limit for the bolometric gamma-ray spectrum. For *Fermi*/GBM, $e_1 = 300 \text{ keV}$ and $e_2 = 50 \text{ keV}$. To be consistent with the inferred bolometric luminosities of those observed LLGRBs, as mentioned in Sec.1, we set $E_1 = 10000 \text{ keV}$ and $E_2 = 1 \text{ keV}$. $n(\varepsilon)$ is the LLGRB prompt photon spectrum, where ε is the photon energy. We assume a broken power-law spectrum similar to that of HLGRBs, expressed by $dn/d\varepsilon = n_b(\varepsilon/\varepsilon_{\gamma b})^{-\beta_1}$ for $\varepsilon < \varepsilon_{\gamma b}$ and $dn/d\varepsilon = n_b(\varepsilon/\varepsilon_{\gamma b})^{-\beta_2}$ for $\varepsilon > \varepsilon_{\gamma b}$. We take $\beta_1 \simeq 1$ at energies below the break and $\beta_2 \simeq 2$ above the break. Then the gamma-ray energy production rate by those LLGRBs that are missed by *Fermi*/GBM can be estimated by

$$\dot{W}_{\gamma, \text{m}} = \frac{1}{\frac{4}{3}\pi(D_{\max}^3 - D_{\min}^3)} \int_{D_{\min}}^{D_{\max}} \int_{L_{\min}}^{L_{\text{lim}}} 4\pi D^2 E_\gamma(L) \frac{dN}{dL} dL dD, \quad (5)$$

where $L_{\text{lim}} = 2.1 \times 10^{46} (D/100 \text{ Mpc})^2 / B(e_1, e_2) \text{ ergs}^{-1}$. Since 40Mpc is the distance of GRB 980425, the closest LLGRB ever detected, while 200Mpc is approximately the attenuation length for iron nuclei of 100EeV, we take $D_{\min} = 40 \text{ Mpc}$ and $D_{\max} = 200 \text{ Mpc}$ as the lower limit and the upper limit of the integration respectively. Due to that $\varepsilon_{\gamma b}$ varies with luminosity, $B(e_1, e_2)$ is a function of the luminosity. We assume that the Yonetoku relation holds for LLGRBs as in the case of GRB 060218 (Yonetoku et al. 2004), i.e. $\varepsilon_{\gamma b} \propto L^{1/2}$, and take $\varepsilon_{\gamma b} = 10 L_{47}^{1/2} \text{ keV}$. We define

$$\mathcal{R} = \dot{W}_{\gamma, \text{m}} / (\dot{W}_\gamma - \dot{W}_{\gamma, \text{m}}), \quad (6)$$

as the ratio between the gamma-ray energy production rates in

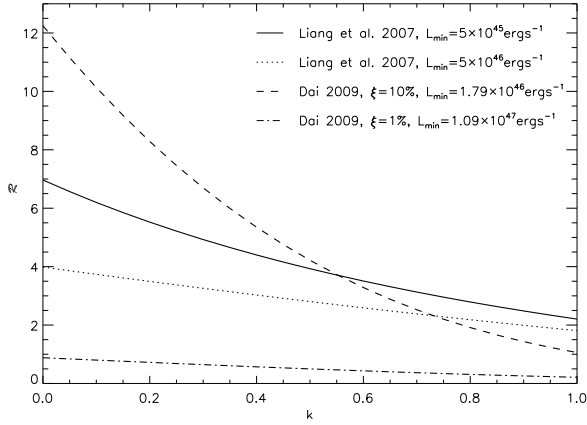


Figure 1. The ratio of the missing to the observable gamma-ray production rate \mathcal{R} changes with the assumed power-law index of the $E_\gamma - L$ relation k ($E_\gamma = 10^{50} L_{47}^k \text{erg}$). Except in the $\xi = 1\%$ case for LFD, the missing gamma-ray energy production rate is several times larger than the observable one.

missing local LLGRBs and that in the observable ones, and present its values in different cases in Table. 1. We find that the gamma-ray energy production rate by missing local LLGRBs constitutes a dominant fraction of the total rate. In some cases, it is larger than that produced by the observable LLGRBs by one order of magnitude. Note that in the $\xi = 1\%$ case of LFD, that \mathcal{R} becomes small is due to an unrealistic high L_{\min} , which is higher than the luminosity of detected LLGRBs (e.g. GRB 980425, GRB 060218). We show how \mathcal{R} changes with k in Fig. 1.

Although the obtained gamma-ray energy production rate is highly dependent on the typical value of E_γ used (i.e. we used $E_\gamma = 10^{50} \text{erg}$ for a LLGRB with luminosity of 10^{47}ergs^{-1}), which could have large uncertainty, the ratio \mathcal{R} is only dependent on $B(e_1, e_2)$, or to be more accurate, the assumed photon spectrum. We also check some other common combinations of β_1, β_2 and $\epsilon_{\gamma b}$ and present the results in Fig. 2. In the region that $L < 10^{47} \text{ergs}^{-1}$, where the missing LLGRBs reside, the value $B(e_1, e_2)$ is generally smaller than 0.3. It is mainly because that the energy window of the detector is so narrow that the spectral peaks for LLGRBs are typically outside of the window.

Recently, Eichler (2011) have shown that the contribution of dim or undetected GRBs to the total all-sky GRB energy flux is small, based on that the cumulative fluence plateaus at a fluence of $\sim 10^{-5} \text{ergcm}^{-2}$, which is much higher than the minimum fluence for both BATSE and *Swift*. However, we note that the trigger threshold for *Swift*/BAT and *Fermi*/GBM is about $10^{-8} \text{ergcm}^{-2} \text{s}^{-1}$ and LLGRBs typical have long duration of $T \sim 10^3 \text{s}$, so LLGRBs with fluence lower than $\sim 10^{-5} \text{ergcm}^{-2}$ would not trigger the detector. Therefore, the plateau only reflects that those GRBs at the low luminosity end of the HLGRB population contribute little to the cumulative fluence (which is actually consistent with the LFs of HLGRBs), irrespective of the LLGRB population. As a distinctly separate class of bursts at very low flux levels, LLGRBs could make a significant contribute to the cumulative fluence only if the detector is significantly more sensitive than *Swift*/BAT and *Fermi*/GBM.

In the internal shock scenario for the gamma-ray emission of LLGRBs, UHECRs are accelerated by the same shocks. So one can

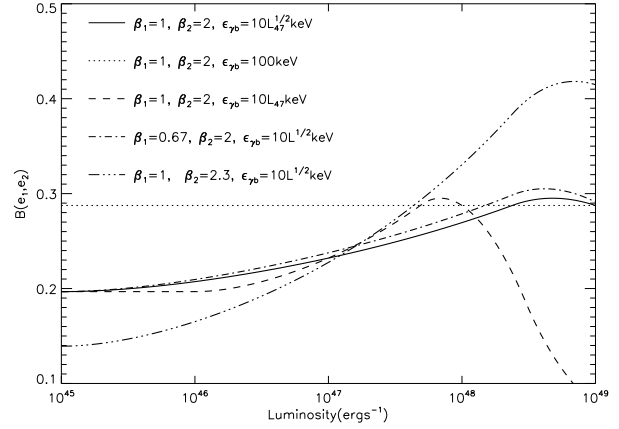


Figure 2. Relation between bandpass ratio $B(e_1, e_2)$ and luminosity with different combinations of parameters of photon spectrum. See text for more discussion.

estimate the energy production rate in UHECRs, assuming some equipartition factors for electrons and protons (nuclei). Assuming a flat spectrum $d\dot{n}/d\varepsilon \propto \varepsilon^{-2}$ for UHECRs, we can now estimate the local UHECRs energy production rate per logarithmic energy interval by LLGRBs

$$\begin{aligned} \dot{W}_{\text{UHECR}}(0) &\equiv \varepsilon^2 \frac{d\dot{n}}{d\varepsilon} \Big|_{\text{UHECR}} = \frac{1}{\ln(\varepsilon_{A,\max}/\varepsilon_{A,\min})} \dot{W}_{\text{CR}}(0) \\ &= \frac{1}{\ln(\varepsilon_{A,\max}/\varepsilon_{A,\min})} \frac{\epsilon_A}{\epsilon_e} \dot{W}_\gamma(0) \end{aligned} \quad (7)$$

where $\dot{W}_{\text{CR}}(0)$ is the local energy production rate for cosmic ray over the whole energy range, $\varepsilon_{A,\min}$ and $\varepsilon_{A,\max}$ are, respectively, the minimum and maximum energies of cosmic rays. Though the value of $\varepsilon_{A,\min}$ is unknown, it is usually assumed that $\ln(\varepsilon_{A,\max}/\varepsilon_{A,\min}) \simeq 10$. Here ϵ_e and ϵ_A are, respectively, the equipartition factors for electrons and protons (nuclei). We adopt the usual values, $\epsilon_e = \epsilon_B = 0.1$ and $\epsilon_A = 1 - \epsilon_e - \epsilon_B$ (ϵ_B is the equipartition factor for the magnetic field), in the following calculation. The results of $\varepsilon^2 \frac{d\dot{n}}{d\varepsilon} \Big|_{\text{UHECR}}$ are given in Table 1 for the two LFs considered. These values are not far from the measured value of the local energy production rate of UHECRs, $(5 \pm 2) \times 10^{43} \text{erg Mpc}^{-3} \text{yr}^{-1}$ (e.g. Katz, Budnik, & Waxman 2009; Waxman 2010), so we conclude that local LLGRBs remain viable sources for UHECRs in terms of the energy production rate.

In the semi-relativistic hypernova scenario for the gamma-ray emission of LLGRBs, UHECR acceleration occurs in the hypernova remnant shock region, which is different from the gamma-ray production region. Nevertheless, the energy production rate in gamma-rays is still a useful indicator, as it reflects a minimum energy production rate in the kinetic energy of the semi-relativistic ejecta, from which the energy of UHECRs is tapped ultimately.

3 UHE NUCLEI FROM LLGRBS

3.1 Acceleration of UHE nuclei

Now we consider the acceleration of nuclei by semi-relativistic hypernova remnant shocks or internal shocks in relativistic shells. For

Table 1. The ratio of gamma-ray energy production rates between the missing local LLGRBs and the observable ones, estimated gamma-ray energy production rate of local LLGRBs and the inferred UHECRs energy production rate in per logarithmic energy interval. See text for more discussion

Luminosity Function	$L_{\min}(10^{47}\text{ergs}^{-1})$	\mathcal{R}^a		$\dot{W}_\gamma(0)^b(10^{43}\text{ergMpc}^{-3}\text{yr}^{-1})$		$\dot{W}_{\text{UHECR}}(0)^c(10^{43}\text{ergMpc}^{-3}\text{yr}^{-1})$	
		k=0	k=1	k=0	k=1	k=0	k=1
Liang et al. (2007)	0.05	7.1	2.2	3.25	2.72	2.60	2.18
Liang et al. (2007)	0.5	4.0	1.8	3.25	3.95	2.60	3.16
Dai (2009) ($\rho_0 = 2000\text{Gpc}^{-3}\text{yr}^{-1}$)	0.18	12.4	1.1	20.0	14.9	16.0	11.9
Dai (2009) ($\rho_0 = 200\text{Gpc}^{-3}\text{yr}^{-1}$)	1.09 ^d	0.89	0.21	2.00	8.42	1.60	6.74

^a : The ratio of gamma-ray energy production rates between the missing local LLGRBs and the observable ones.

^b : The total (the missing + the observable) gamma-ray energy production rate of local LLGRBs.

^c : The inferred local UHECRs energy production rate in per logarithmic energy interval, see Eq. (7)

^d : Since the luminosities of GRB 980425 and GRB 060218 are less than this value by a factor of 2–4, this case may be largely different from the reality. We just show them here for reference.

Fermi shock acceleration, the characteristic acceleration timescale is $t_{\text{acc}} = \lambda c / \beta_{\text{sh}}^2$, where $\lambda = \eta R_L$ is the scattering mean free path, R_L is the Larmor radius of particles and $\beta_{\text{sh}} c$ is the shock speed. Here $\eta \sim a$ few, describes the ratio between the acceleration time and Larmor time ($\eta = 1$ corresponds to the efficient Bohm diffusive shock acceleration). For a nucleus of mass Am_p and charge Ze , the time needed to accelerate it to the observed energy of ϵ_A in the comoving frame is $t_{\text{acc}} = \eta \epsilon_A / (Ze B \Gamma \beta_{\text{sh}}^2 c)$. Cooling of particles restricts the maximum energy. Adiabatic expansion and synchrotron emission are two important cooling mechanisms. The cooling time of the former one is given by $t_{\text{ad}} \approx t_{\text{dyn}} \approx R_{\text{sh}} / \Gamma \beta_{\text{sh}} c$, where R_{sh} is the radius of shock acceleration site and Γ is the bulk Lorentz factor of the shock, while the latter one is $t_{\text{syn}} = \frac{6\pi m_A c}{(Z^4 \sigma_T m_e^2 / m_A^2) \gamma_A B^2}$, where σ_T is Thomson scattering cross section for electrons and $\sigma_T(\frac{m_e^2}{m_A^2}) Z^4$ is the corresponding cross section for nucleus with Ze charge and Am_p mass.

3.1.1 Semi-relativistic hypernova scenario

Whether particles can be accelerated to ultra-high energies in the hypernova scenario has been discussed in Wang, Razzaque, & Mészáros (2008), in which a distribution of the ejecta energy with ejecta velocity has been assumed. Here for simplicity we only focus on the semi-relativistic part of the ejecta, whose velocity is $\Gamma \beta \gtrsim 0.5$. According to the simulation of hypernova explosion such as SN1998bw by MacFadyen, Woosley, & Heger (2001), the isotropic-equivalent kinetic energy of ejecta is roughly constant at angles larger than 20° , so we assume a spherical hypernova ejecta expanding into the circum-stellar wind medium. Particles are accelerated in the region where the ejecta is freely expanding before being decelerated by the swept-up circum-stellar medium. The size of this free-expansion phase region for ejecta of a particular velocity $\beta_{\text{sh}} c$ and kinetic energy E_K is

$$R_{\text{HN}} \approx 4 \times 10^{17} E_{K,51} (\Gamma \beta_{\text{sh}})^{-2} \dot{M}_{-5}^{1/2} v_{w,3}^{-1/2} \text{cm}, \quad (8)$$

which is much larger than the radius at which gamma-ray photons of LLGRBs are produced (Wang et al. 2007b), where $\dot{M} = 10^{-5} \dot{M}_{-5} \text{M}_\odot \text{yr}^{-1}$ is the wind mass loss rate, whose average value is $3 \times 10^{-5} \text{M}_\odot \text{yr}^{-1}$ for WR stars, and $v_w = 10^3 v_{w,3} \text{km s}^{-1}$ is the wind velocity (Willis 1991; Chevalier & Li 1999). During the free expansion phase, the magnetic field energy density is $B^2/8\pi = 2\epsilon_B \rho_w (R_{\text{HE}})^2 \beta_{\text{sh}}^2$, where $\epsilon_B = 0.1 \epsilon_{B,-1}$ is the fraction of the equipartition value of the magnetic field energy and ρ_w is the mass density of the stellar wind at radius R_{HN} . The magnetic field at the free-expansion radius R_{HN} is

$$B = 0.5 \epsilon_{B,-1}^{1/2} R_{\text{HN},17}^{-1} \beta_{\text{sh}} \dot{M}_{-5}^{1/2} v_{w,3}^{-1/2} \text{G}. \quad (9)$$

From $t_{\text{acc}} = t_{\text{dyn}}$, the maximum energy is

$$\epsilon_{A,\text{max}} \approx Ze B R_{\text{HE}} \beta_{\text{sh}} / \eta = 5.2 \times 10^{20} \eta^{-1} \left(\frac{Z}{26} \right) \epsilon_{B,-1}^{1/2} \beta_{\text{sh}}^2 \dot{M}_{-5}^{1/2} v_{w,3}^{-1/2} \text{eV}. \quad (10)$$

Note that the synchrotron loss of UHE nuclei in the semi-relativistic hypernova scenario is much lower than the adiabatic loss, so it is not considered here.

3.1.2 Internal shock scenario

In the internal shock scenario, the magnetic field B can be estimated by $B^2/8\pi = \epsilon_B U = \frac{\epsilon_B}{\epsilon_e} U_\gamma$ as all the energies of electrons are almost lost into radiation, where U is the comoving thermal energy density and $U_\gamma = L/4\pi R_{\text{sh}}^2 \Gamma^2 c$ is the comoving gamma-ray energy density for an internal shock radius of R_{sh} . So,

$$B = \left(\frac{2\epsilon_B L}{\epsilon_e c} \right)^{1/2} \frac{1}{\Gamma R_{\text{sh}}} = 4.30 \times 10^2 \epsilon_{e,-1}^{-1/2} \epsilon_{B,-1}^{1/2} L_{47}^{1/2} \Gamma_1^{-3} \delta t_2^{-1} \text{G} \quad (11)$$

where $R_{\text{sh}} = 2\Gamma^2 c \delta t$ has been used and δt is the variability time.

The maximum nucleus energy is determined by equating t_{acc} with the smaller one of the two cooling timescales t_{ad} and t_{syn} . We have

$$\epsilon_{A,\text{max}} = 2.0 \times 10^{21} \eta^{-1} \left(\frac{Z}{26} \right) \epsilon_{e,-1}^{-1/2} \epsilon_{B,-1}^{1/2} L_{47}^{1/2} \Gamma_1^{-1} \beta_{\text{int}} \text{eV} \quad (12)$$

for $t_{\text{acc}} = t_{\text{dyn}}$, and

$$\varepsilon_{A,\text{max}} = 2.3 \times 10^{21} \eta^{-1/2} \left(\frac{A}{56}\right)^2 \left(\frac{Z}{26}\right)^{-3/2} \epsilon_{e,-1}^{1/4} \epsilon_{B,-1}^{-1/4} L_{47}^{-1/4} \Gamma_1^{5/2} \delta t_2^{1/2} \beta_{\text{int}} \text{eV} \quad (13)$$

for $t_{\text{acc}} = t_{\text{syn}}$. From Eq. (12), one can derive a minimum luminosity for LLGRBs that can accelerate nuclei to ultra high energies, i.e.

$$L_{\text{min,acc}} = 2.5 \times 10^{44} \varepsilon_{A,100\text{EeV}}^2 \eta^2 \left(\frac{Z}{26}\right)^{-2} \epsilon_{e,-1} \epsilon_{B,-1}^{-1} \Gamma_1^2 \beta_{\text{int}}^{-2} \text{ergs}^{-1}. \quad (14)$$

According to Eq. (13), there is also a maximum luminosity for LLGRBs that can accelerate nuclei to ultra high energies, i.e.

$$L_{\text{max,acc}} = 2.8 \times 10^{52} \varepsilon_{A,100\text{EeV}}^{-4} \eta^{-2} \left(\frac{A}{56}\right)^4 \left(\frac{Z}{26}\right)^{-6} \epsilon_{e,-1} \epsilon_{B,-1}^{-1} \Gamma_1^{10} \delta t_2^4 \beta_{\text{int}}^4 \text{ergs}^{-1} \quad (15)$$

The steep dependence on the bulk Lorentz factors Γ results from the steep dependence of the magnetic field energy on Γ in the internal shock assumption. If the luminosity is too high, the radiative cooling is so rapid that these nuclei can not reach ultrahigh energies. As the minimum luminosity adopted in Sec.2 is higher than $L_{\text{min,acc}}$, we conclude that even those missing LLGRBs are powerful enough to accelerate UHECRs. Since the internal shock is mildly relativistic with $\beta_{\text{int}} \approx 1$, hereafter, we drop the dependence on β_{int} in our analytical calculation.

3.2 Survival of UHE nuclei

UHE nuclei will suffer from photo-disintegration and photopion loss by interactions with low-energy photons in the sources. For UHE nuclei, photo-disintegration is usually more important (Wang, Razzaque, & Mészáros 2008; Allard et al. 2008). Now we study whether UHE nuclei accelerated in LLGRBs can survive in the semi-relativistic hypernova scenario and internal shock scenario.

3.2.1 Semi-relativistic hypernova scenario

There are two photon sources which could cause photo-disintegration of heavy nuclei: one is provided by hypernova thermal photons from radioactive elements of the hypernova ejecta, and another is provided by the synchrotron photons from the hypernova remnant shock. The free-expansion time for the semi-relativistic ejecta is

$$t = \frac{R_{\text{HE}}}{\Gamma \beta_{\text{sh}} c} \simeq 1.3 \times 10^7 E_{k,51} (\Gamma \beta_{\text{sh}})^{-3} \dot{M}_{-5}^{1/2} v_{w,3}^{-1/2} \text{s}. \quad (16)$$

At earlier times when the fast semi-relativistic ejecta is decelerated, the flux from the hypernova thermal photons is expected to be dominated. We use the luminosity of SN1998bw as a representative for the hypernova luminosity of thermal photons. At time $t \sim 100$ days after the burst, the optical luminosity of SN1998bw drops to the level of about $L_{\text{HE}} \sim 10^{41} \text{ergs}^{-1}$ (Sollerman et al. 2002). A nucleus of energy $E = 10^{20} \text{eV}$ interacts with target photons with a threshold energy $\varepsilon_{\text{th}} \gtrsim 0.01(A/56)E_{20}^{-1} \text{eV}$. A rough estimate of the optical depth of photo-disintegration of UHE nuclei (losing one nucleon) due to hypernova thermal photons is

$$\tau \lesssim \sigma_{\text{GDR}} \left(\frac{L_{\text{HN}}}{4\pi R_{\text{HN}}^2 c \varepsilon_{\text{HN}}} \right) \left(\frac{R_{\text{HN}}}{\varrho} \right) = 3 \times 10^{-2} \left(\frac{A}{56} \right) L_{\text{HN},41} R_{\text{HN},17}^{-1} \left(\frac{\varepsilon_{\text{HN}}}{1 \text{eV}} \right)^{-1}, \quad (17)$$

where $\sigma_{\text{GDR}} = 1.45 \times 10^{-27} \text{Acm}^2$ is the peak cross section of the Giant Dipole Resonance (GDR), $\varrho \simeq 4$ is the compression ratio of the hypernova remnant shock and $\varepsilon_{\text{HE}} \simeq 1 \text{eV}$ is the characteristic energy of hypernova thermal photons.

3.2.2 Internal shock scenario

1. Photon Spectrum

The photon spectrum of the prompt emissions of GRBs can be approximately described by a broken power-law. In the comoving frame of the relativistic outflow, it can be described as

$$n(\varepsilon_\gamma) = n_b \begin{cases} (\varepsilon/\varepsilon_{\gamma b}^{\text{co}})^{-\beta_1}, & \varepsilon < \varepsilon_{\gamma b}^{\text{co}}, \\ (\varepsilon/\varepsilon_{\gamma b}^{\text{co}})^{-\beta_2}, & \varepsilon_{\gamma b}^{\text{co}} < \varepsilon < \varepsilon_{\text{max}}. \end{cases} \quad (18)$$

where $\varepsilon_{\gamma b}^{\text{co}}$ is the break energy in the comoving frame. As we did in Sec.2, we take $\beta_1 = 1$ and $\beta_2 = 2$ as typical values. At low energy region, in the framework of the internal shock model, there may be another spectral break, i.e. the synchrotron self-absorption (SSA) break.

Now we estimate the SSA break energy for LLGRBs. The two characteristic break frequencies in the synchrotron spectrum in the comoving frame are given by

$$\nu_m = 1.02 \times 10^{12} f(p) \Gamma_1^{-3} \delta t_2^{-1} \epsilon_{e,-1}^{3/2} \epsilon_{B,-1}^{1/2} L_{47}^{1/2} (\gamma_{\text{int}} - 1)^2 \text{Hz} \quad (19)$$

and

$$\nu_c = 2.37 \times 10^9 \Gamma_1^7 \delta t_2 \epsilon_{e,-1}^{3/2} \epsilon_{B,-1}^{-3/2} L_{47}^{-3/2} (1 + Y)^{-2} \text{Hz}, \quad (20)$$

where $f(p) = 6(p-2)/(p-1)$, γ_{int} is the Lorentz factor of the internal shock, and Y is the Compton parameter for inverse Compton loss. In the fast cooling regime ($\nu_c < \nu_m$), $Y = \frac{-1 + \sqrt{1 + 4\epsilon_e/\epsilon_B}}{2} \approx 0.6$ for $\epsilon_e = \epsilon_B = 0.1$. Since it is less than unity, we just neglect its influence on the value of ν_c . The SSA coefficient in fast cooling regime can be estimated by (Wu et al. 2003)

$$k_\nu = \begin{cases} \frac{c_0 e}{B \gamma_c^2} n_e \left(\frac{\nu}{\nu_c} \right)^{-5/3}, & \nu < \nu_c \\ \frac{c_0 e}{B \gamma_c^2} n_e \left(\frac{\nu}{\nu_c} \right)^{-3}, & \nu_c < \nu < \nu_m \\ \frac{c_0 e}{B \gamma_m^2} \frac{\gamma_c}{\gamma_m} n_e \left(\frac{\nu}{\nu_m} \right)^{-(p+5)/2}, & \nu_m < \nu \end{cases} \quad (21)$$

where γ_m and γ_c is the minimum Lorentz factor and cooling Lorentz factor, n_e is the number density of electrons and $c_0 \sim 15$ is a constant. The SSA frequency is determined by $k_\nu \Delta R_{\text{co}} = 1$, where ΔR_{co} is the length of the shock region in the comoving frame. ΔR_{co} is related to the column density of electrons Σ by

$$\Sigma = n_e \Delta R_{\text{co}} = \frac{N_{\text{shell}}^e}{4\pi R_{\text{int}}^2} \quad (22)$$

where $N_{\text{shell}}^e = \frac{L \delta \gamma_{\text{int}}}{\epsilon_e (\gamma_{\text{int}} - 1) \Gamma m_A c^2} \frac{Z}{\Gamma m_A c^2}$ is the total number of electrons in the colliding shell. Finally, we get the SSA frequency in the comoving frame, i.e.

$$\varepsilon_{\text{SSA}} = 0.012 \Gamma_1^{-13/6} \delta t_2^{-13/18} L_{47}^{13/36} \text{eV} \quad (23)$$

for $\epsilon_e = 0.1$, $\epsilon_B = 0.1$, $\gamma_{\text{int}} = 2$ and $p = 2.2$.

Since $\nu_{\text{SSA}} > \nu_m$, the SSA coefficient is $\propto \varepsilon^{-3.6}$ for $p = 2.2$ according to Eq. (21), hence the spectral index below the SSA frequency is -2.6 . Thus, the photon spectrum in the comoving frame

is

$$n(\epsilon) = n_b \begin{cases} (\epsilon_{\text{SSA}}/\epsilon_{\gamma b}^{\text{co}})^{-1} (\epsilon/\epsilon_{\text{SSA}})^{2.6}, & \epsilon < \epsilon_{\text{SSA}} \\ (\epsilon/\epsilon_{\gamma b}^{\text{co}})^{-1}, & \epsilon_{\text{SSA}} < \epsilon < \epsilon_{\gamma b}^{\text{co}} \\ (\epsilon/\epsilon_{\gamma b}^{\text{co}})^{-2}, & \epsilon_{\gamma b}^{\text{co}} < \epsilon < \epsilon_{\text{max}} \end{cases} \quad (24)$$

2. Photodisintegration

For an UHE nucleus with energy ϵ_A in the observer frame, the fractional photo-disintegration rate is

$$t_{\text{dis},f}^{-1}(\gamma_A) = \frac{1}{A} \left| \frac{dA}{dt} \right| = \frac{c}{2\gamma_A^2} \int_{\epsilon_{\text{th}}}^{\infty} d\epsilon \sigma_{\text{dis}}(\epsilon) \epsilon \int_{\epsilon/2\gamma_A}^{\infty} dx x^{-2} n(x) \quad (25)$$

where $\gamma_A = \epsilon_A/\Gamma m_A c^2 = 1.9 \times 10^8 (A/56)^{-1} \Gamma_1^{-1} \epsilon_{A,100\text{EeV}}$, $\sigma_{\text{dis}}(\epsilon)$ is the photo-disintegration total cross section, ϵ is the photon energy in the nucleus rest frame and ϵ_{th} is the threshold energy. This rate can be calculated numerically with the cross section given in Puget, Stecker, & Bredekamp (1976). But as an estimate we can approximate the cross section mainly contributed by the giant dipole resonance (GDR) and show the numerical results later. The peak cross section due to GDR is $\sigma_{\text{GDR}} = 1.45 \times 10^{-27} \text{Acm}^2$ and $\epsilon_{\text{GDR}} = 42.65 A^{-0.21} \text{MeV}$ (for $A > 4$) with a width $\Delta_{\text{GDR}} = 8 \text{MeV}$. We find that the energy of the photons that interact with UHE nuclei via GDR resonance is about $\epsilon_{\text{GDR}}^{\text{co}} \sim 0.2 \Gamma_1 (A/56)^{0.79} (\epsilon_{A,50\text{EeV}})^{-1} \text{eV}$ in the comoving frame, which is larger than the SSA frequency, so the SSA process in the low-energy photons will have little influence on photo-disintegration process for these representative parameters. Approximating the integral by the contribution from the resonance, the fractional photo-disintegration rate is

$$t_{\text{dis},f}^{-1} = \frac{U_\gamma}{4\epsilon_{\gamma b}^{\text{co}}} \frac{c\sigma_{\text{GDR}}\Delta_{\text{GDR}}}{A\epsilon_{\text{GDR}}} \begin{cases} (\epsilon_A/\epsilon_{\text{Ab}})^{\beta_1-1} & \epsilon_A > \epsilon_{\text{Ab}} \\ (\epsilon_A/\epsilon_{\text{Ab}})^{\beta_2-1} & \epsilon_A < \epsilon_{\text{Ab}} \end{cases} \quad (26)$$

where $U_\gamma \approx n_b(\epsilon_b^{\text{co}})^2 [1 + \ln(\epsilon_{350\text{keV}}/\epsilon_{\gamma b})] \approx 4n_b(\epsilon_{\gamma b}^{\text{co}})^2$ is the energy density of photons in the comoving frame in the energy window of *Swift*/BAT and $\epsilon_{\text{Ab}} = 0.5\epsilon_{\text{GDR}}m_A c^2/\epsilon_{\gamma b} \approx 1.5 \times 10^{15} A \Gamma_1^2 \epsilon_{\gamma b,10\text{keV}}^{-1} \text{eV}$ is the nuclei break energy in the observer frame. For UHE nuclei, we have $\epsilon_A \gg \epsilon_{\text{Ab}}$, then the effective optical depth for photo-disintegration is

$$\tau_{\text{dis},f} = \frac{t_{\text{dyn}}}{t_{\text{dis},f}} = 0.043 \frac{L_{47}(A/56)^{0.21}}{\Gamma_1^4 \delta t_2 \epsilon_{\gamma b,10\text{keV}}} \quad (27)$$

for $\beta_1 = 1$. Thus we can see that a larger break energy, a larger bulk Lorentz factor or a smaller luminosity will be favourable for the survival of UHE heavy nuclei. We note that these quantities in GRBs may have inherent correlations.

This motivates us to study in which kind of bursts UHE nuclei can survive, especially whether UHE nuclei can survive in those missing, dim LLGRBs, when these inherent correlations are taken into account. For the break energy $\epsilon_{\gamma b}$, we still assume that the Yonetoku relation holds for LLGRBs, i.e. $\epsilon_{\gamma b} \propto L^{1/2}$. As to Γ , assuming the break energy of the spectrum in the comoving frame are constant for all LLGRBs², we have $\Gamma \propto \epsilon_{\gamma b}$ and hence $\Gamma \propto L^{1/2}$. The variability time scale δt may depend on the central engine activity and we simply fix its value to 100s. Under these assumptions, we have $\tau_{\text{dis},f} \propto L^{-3/2}$, and consequently, UHE heavy nuclei can

² Given that LLGRBs have lower break energies than HLGRBs, and on the other hand, LLGRBs are suggested to arise from less relativistic jets Soderberg et al. (2006); Toma et al. (2007), the intrinsic range of the break energy in the comoving frame could be small.

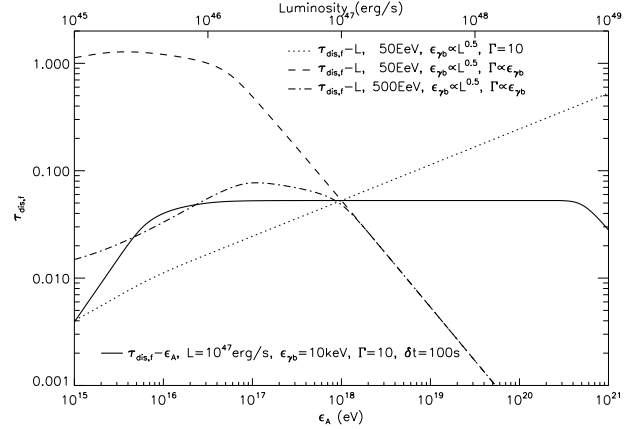


Figure 3. The fractional optical depth for photodisintegration of iron nuclei in the internal shock scenario. It is a function of the energy of nuclei (the solid line) and is a function of the luminosity of LLGRBs (dashed lines). The parameters used in the calculation are given in the figure for each line. See text for more details.

survive more easily in LLGRBs with relatively high luminosities. The main reason for this is that LLGRBs with lower luminosity may have smaller internal shock radii for a fixed δt and hence a higher density of target photons. On the other hand, if we assume that Γ is a constant for LLGRBs, we will obtain $\tau_{\text{dis},f} \propto L^{1/2}$. In this case, UHE heavy nuclei can survive more easily in LLGRBs with relatively low luminosities.

The SSA break may affect the photo-disintegration rate when $\epsilon_{\text{GDR}}^{\text{co}} < \epsilon_{\text{SSA}}$, because the number of photons that can interact with the heavy nuclei via GDR is considerably reduced by the SSA process. This is applicable for nucleus at the highest energy (i.e. typically above a few times 10^{20}eV). In the SSA regime, we have

$$t_{\text{dis},f}^{-1} \approx \frac{U_\gamma}{12.8\epsilon_{\gamma b}^{\text{co}}} \frac{c\epsilon_{\text{GDR}}\sigma_{\text{GDR}}\Delta_{\text{GDR}}}{A\gamma_A^2 \epsilon_{\text{SSA}}} \quad (28)$$

The effective photo-disintegration optical depth is

$$\tau_{\text{dis},f}(\epsilon_A) = 0.039 \frac{L_{47}^{5/18} (A/56)^{1.79}}{\Gamma_1^{-7/3} \delta t_2^{-4/9} \epsilon_{\gamma b,10\text{keV}} (\epsilon_{A,500\text{EeV}})^2}. \quad (29)$$

If we assume $\epsilon_{\gamma b} \propto L^{1/2}$ and $\Gamma \propto \epsilon_{\gamma b}$, we will have $\tau_{\text{dis},f} \propto L^{17/18}$, hence UHE heavy nuclei can survive from photo-disintegration more easily in LLGRBs with relatively low luminosities, if the energy of the effective target photons falls below the SSA break energy.

In Fig.3, we show the effective fractional photo-disintegration optical depth $\tau_{\text{dis},f}$ for iron nucleus, calculated according to Eq. (25) and using the cross section described by the Lorentzian form in the energy range $\epsilon_{\text{th}} < \epsilon < 30 \text{MeV}$ and a flat cross section for multi-nucleon loss in the energy range $30\text{MeV} < \epsilon < 150\text{MeV}$ (Puget, Stecker, & Bredekamp 1976; Karakula & Tkaczyk 1993). From the solid line, one can see that $\tau_{\text{dis},f}$ is almost independent of the energy of nucleus ϵ_A when $\epsilon_A > \epsilon_{\text{Ab}}$ (see the approximate analytic estimate in Eq. (27)). When the energy of the nucleus becomes larger than several times 10^{20}eV , the nucleus starts to interact with target photons with energies below the SSA break so that the effective optical depth decreases with the energy of nucleus. Fig. 3 (the dotted, dashed and dash-dotted lines) also describes how $\tau_{\text{dis},f}$ of

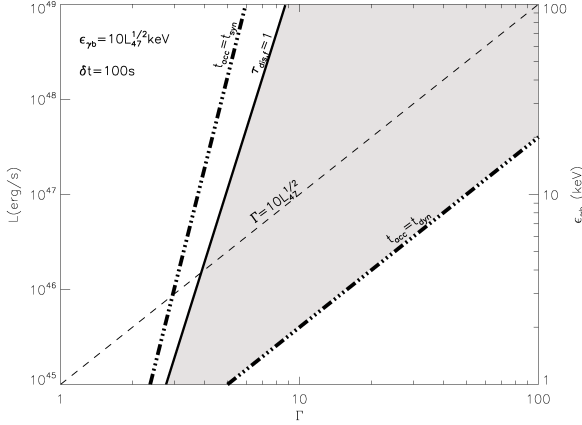


Figure 4. The parameter space of luminosity L and Lorentz factor Γ in the internal shock scenario. The hatched area is the parameter space of L and Γ of LLGRBs in which iron nuclei of energy 50 EeV can both be accelerated and survive in the sources. The thick solid line represents the condition $\tau_{\text{dis},f} = 1$. The area between the two thick dash-dotted lines represent the parameter space in which iron nuclei can be accelerated to 50 EeV. Also shown is the Yonetoku's relation for GRBs (the thin dashed line).

an UHE nucleus with a fixed energy depends on the luminosity of LLGRB. We can see that under the assumptions of $\epsilon_{yb} \propto L^{1/2}$ and $\Gamma \propto \epsilon_{yb}$, UHE nuclei tend to survive in LLGRB with relative high luminosity. The relation between $\tau_{\text{dis},f}$ and ϵ_A in the assumption that Γ is a constant for all LLGRBs is also presented in Fig. 3 for comparison. In this case, UHE nuclei survive more easily in LLGRB with lower luminosity.

In Fig. 4, we show the parameter space (denoted by the hatched area) of L and Γ in which iron nucleus can be accelerated to 50 EeV and can escape from the source with most of its initial nucleons preserved meanwhile. It shows that LLGRBs with larger L tend to satisfy both constraints in the internal shock scenario. Nevertheless, $\tau_{\text{dis},f} \simeq 1$ occurs at $L \simeq 10^{46} \text{ erg s}^{-1}$, which is sufficiently low that most LLGRBs we are concerning are within the safety limit.

4 NEUTRINO BACKGROUND FROM LLGRBS

UHE nuclei will interact with low-energy photons in the sources and produce high-energy neutrinos. Hence neutrino detection is a useful tool for probing the acceleration of UHECRs in sources. In the semi-relativistic hypernova scenario, the production of neutrinos is mainly through the photomeson interactions of UHE nuclei with hypernova thermal photons (Wang et al. 2007a). It has been found that the diffuse neutrino flux contributed by semi-relativistic hypernova is too low to be detected by cubic kilometer detectors such as Icecube (Wang et al. 2007a).

In internal shock scenario, the production of neutrinos is mainly through the photomeson interactions of UHE nuclei with low-energy prompt photons in LLGRBs. The fractional energy loss rate of a nucleus with energy ϵ_A in the comoving frame due to pho-

tomeson productions is

$$t_{\text{mes}}^{-1}(\gamma_A) = \frac{1}{\gamma_A} \left| \frac{d\gamma_A}{dt} \right|_{\text{mes}} = \frac{c}{2\gamma_A^2} \int_{\epsilon_{\text{th}}}^{\infty} d\epsilon \sigma_{\text{mes}}(\epsilon) \xi_A(\epsilon) \epsilon \int_{\epsilon/2\gamma_A}^{\infty} dx x^{-2} n(x) \quad (30)$$

where ϵ is the photon energy in the rest frame of the nucleus, $\epsilon_{\text{th}} = 0.15 \text{ GeV}$ is the threshold photon energy for photomeson interaction, $\sigma_{\text{mes}}(\epsilon)$ is the cross section of photomeson production and $\xi_A(\epsilon)$ is the average fraction of energy lost to secondary pions. Above the threshold energy, the main contribution of pion production is due to the Δ resonance at $\epsilon_{\Delta} = 0.34 \text{ GeV}$, for which the cross section can be approximately by a Lorentzian form (e.g. Mücke et al. 2000). Neglecting the nuclear shadowing effect in photoproduction (Michalowski et al. 1977), the peak cross section is $\sigma_{\Delta} \simeq \sigma_{py} A \simeq 4.1 \times 10^{-28} \text{ A cm}^2$ (Anchordoqui et al. 2008; Murase et al. 2008), where σ_{py} is the peak cross section for protons. As $\xi_A(\epsilon) \sim \xi_p(\epsilon)/A$, $\sigma_{\Delta} \xi_A$ is independent of A . The energy of the photons that interact with UHE nuclei via Δ resonance is $\epsilon_{\Delta}^{\text{co}} \sim 3.8 \Gamma_1 (A/56) (\epsilon_{A,50 \text{ EeV}})^{-1} \text{ eV}$ in the comoving frame. Since this energy is much larger than the SSA break energy, the SSA process has little effect on the photomeson process, even for the nucleus with energy of a few times 10^{20} eV . Approximating the integral by the contribution from the resonance, the total fraction of energy lost by nuclei to pions is

$$f_{\pi}(\epsilon_A) = \frac{t_{\text{dyn}}}{t_{\text{mes}}} = \frac{R_{\text{int}}}{\Gamma c t_{\text{mes}}} \simeq 0.004 \frac{L_{47}}{\epsilon_{yb,10 \text{ keV}} \Gamma_1^4 \delta t_2}. \quad (31)$$

So $f_{\pi}(\epsilon_A)$ depends on the inherent relations among Γ , ϵ_{yb} and L . For $\epsilon_{yb} \propto L^{1/2}$ and $\Gamma \propto \epsilon_{yb}$, we have $f_{\pi}(\epsilon_A) \propto L^{-3/2}$. But in the case that the bulk Lorentz factor is a constant with $\Gamma = 10$, $f_{\pi}(\epsilon_A) \propto L^{1/2}$. For LLGRBs with luminosity in the range of $L \sim 10^{46-49} \text{ erg s}^{-1}$, $f_{\pi} \ll 1$ for both cases, which indicates that most heavy nuclei suffer from negligible energy loss due to photomeson production process.

The diffuse neutrino flux contributed by all LLGRBs can be obtained through the integration over the whole luminosity range of LLGRBs, which is

$$\epsilon_v^2 \frac{dN_v}{d\epsilon_v}(\epsilon_v) = \frac{1}{4} \frac{c}{4\pi H_0} f_z \int_{L_{\text{min}}(\epsilon_A)}^{L_{\text{max}}} \min[1, f_{\pi}(L)] \epsilon_A^2 \frac{dN_A}{d\epsilon_A} \zeta_{\pi} \frac{dN}{dL} dL \quad (32)$$

where $f_z \sim 3$ is the correction factor for the contribution from high redshift sources and f_{π} is the suppression factor on the neutrino flux due to pion cooling (Rachen & Mészáros 1998; Razzaque, Mészáros, & Waxman 2004; Wang & Dai 2009). Since the synchrotron cooling dominates the cooling process, we have $\zeta_{\pi} = \tau_{\pi}^{-1} / (t_{\pi, \text{syn}}^{-1} + \tau_{\pi}^{-1})$, where $t_{\pi, \text{syn}} = 12 L_{47}^{-1} \Gamma_1^7 \delta t_2^2 (\epsilon_{\pi, 1 \text{ EeV}})^{-1} \text{ s}$ is the synchrotron cooling time and $\tau_{\pi} = 2.6 \times 10^{-8} \gamma_{\pi} = 186 \epsilon_{\pi, 1 \text{ EeV}} \text{ s}$ is the lifetime of pions. The lower limit of the integral $L_{\text{min}}(\epsilon_A)$ is given in Table. 1. The results obtained numerically are shown in Fig. 5 for the two LFs. It shows that only in the case of high local rate of LLGRBs, there is a chance that diffuse neutrinos from LLGRBs could be detected by cubic kilometer detectors such as Icecube.

5 DISCUSSIONS AND CONCLUSIONS

The origin of heavy or intermediate-mass nuclei in LLGRBs remains to be an open issue. In the hypernova remnant scenario, cosmic ray particles originate from the material swept-up by the

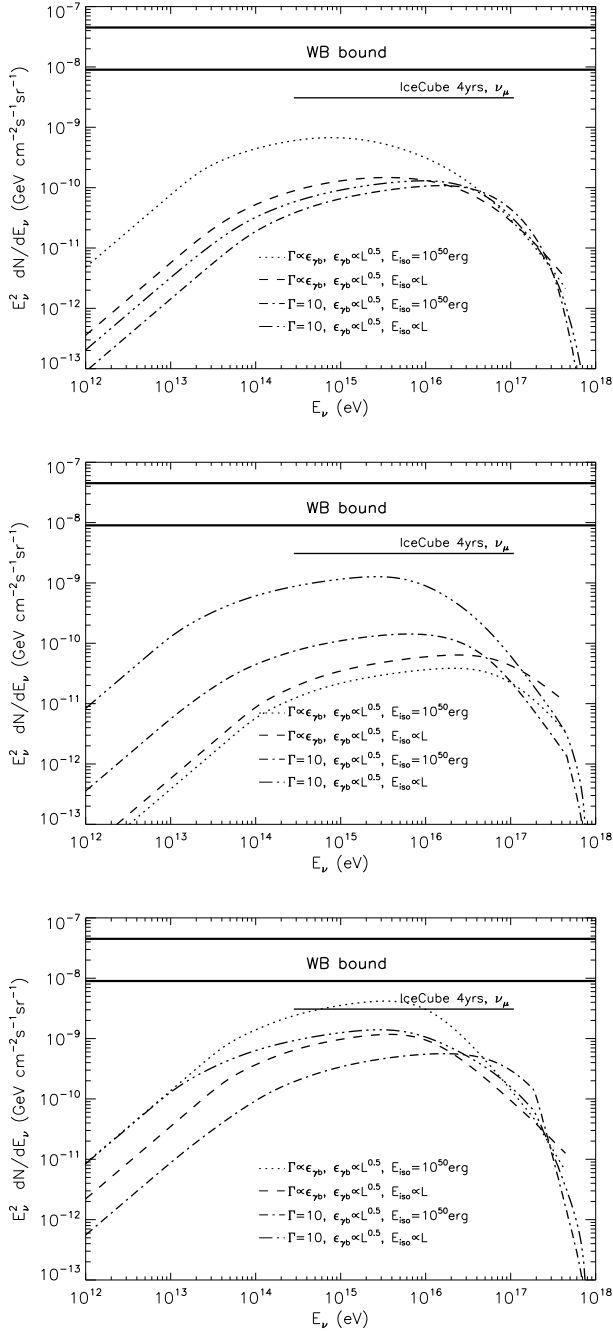


Figure 5. The diffuse neutrino background from LLGRBs. The top panel is for the LF in Liang et al. (2007), whereas the middle and the bottom ones are for the LF in Dai (2009), but for a local rate of $\rho_0 = 200 \text{ Gpc}^{-3} \text{ yr}^{-1}$ and $\rho_0 = 2000 \text{ Gpc}^{-3} \text{ yr}^{-1}$ respectively. The reference values of $\epsilon_{\gamma b}$, Γ and $E_{\gamma, \text{iso}}$ in the scalings are 10 keV, 10 and 10^{50} erg respectively for a LLGRB with luminosity of $10^{47} \text{ erg s}^{-1}$. We also plot the IceCube sensitivity to diffuse neutrino fluxes in 4 years operation (Spiering 2008) and the Waxman-Bahcall bounds (Waxman & Bahcall 1999).

semi-relativistic hypernova shock front. The progenitors of hypernovae are thought to be Wolf-Rayet stars, as the spectral type of the discovered supernovae in these events is typically Ic. These stars are stripped of their hydrogen envelope and sometimes even the helium envelope, so the circum-stellar wind is rich of heavy elements, such as C and O. Thus, heavy or intermediate-mass UHE nuclei may naturally originate from the element-enriched stellar wind of Wolf-Rayet stars in the hypernova scenario. In WC type Wolf-Rayet stars, the C abundance is $X_C \approx 20\% - 55\%$ (by mass) and the O abundance is $X_O \approx 5\% - 10\%$ (Crowther 2007). In WO type Wolf-Rayet stars, O and C abundances are even higher, with $X_C \approx 40\% - 55\%$ and $X_O \approx 15\% - 25\%$ (e.g. Kingsburgh, Barlow, & Storey 1995). The abundances of these elements are clearly much higher than the solar values. In the internal shock scenario for LLGRBs, the origin of nuclei is, however, quite uncertain. The uncertainty lies in whether there are nuclei entrained into the relativistic jet during the formation of the jet out of the collapsing core of massive stars. The temperature of the accretion disk resulted from the collapsing core needs to be sufficiently low that nuclei in the disk will not be photo-disintegrated by the disk thermal photons. This condition may be satisfied if the accretion rate for LLGRBs is sufficiently low. Another possibility for the origin of nuclei in the internal shock scenario is that nuclei present in the surrounding stellar envelope are entrained into the jet while jet is propagating through the stellar envelope. The validity of this possibility needs a detailed numerical simulation of the jet propagation in LLGRBs.

In this paper, we have suggested that many dim local low luminosity GRBs may be missed by *Fermi*/GBM and these missing LLGRBs could make a dominant contribution to observed flux of UHECRs. If true, it can relieve partly the discrepancy between the energy production rate in UHECRs and that in gamma-ray photons recorded by *Fermi*/GBM, as raised by Eichler et al. (2010). We first calculate the energy production rate in gamma-ray photons by LLGRBs as a separate population from high-luminosity GRBs and estimate how large those missing LLGRBs contribute to the total gamma-ray energy production. In the calculation, we take two different LFs for LLGRBs that were proposed in the literatures. We find that the gamma-ray energy production rate by LLGRBs for both LFs are one to two orders of magnitude larger than that estimated by Eichler et al. (2010). The missing part of the energy production rate in gamma-rays could account for a fair proportion or even the vast majority of the total one and hence could be much larger than the observable part. It should be noted that our results depend on many assumptions, such as the form of LF, the spectrum of LLGRBs and some inherent relations among parameters of LLGRBs (e.g. $E_\gamma - L$ relation, $\epsilon_{\gamma b} - L$ relation). To get a more accurate results, further studies in these relations with larger statistics are needed.

There are two scenarios for the UHECR acceleration in LLGRBs, one is the semi-relativistic hypernova scenario where UHECRs are accelerated by the semi-relativistic hypernova shock expanding into the circum-stellar wind and another is the internal shock scenario where UHECRs are accelerated by internal shocks within the variable relativistic outflow. We find that, in both scenarios, only intermediate-mass or heavy nuclei could be accelerated to energies above 10^{20} eV, which is consistent with the recent findings of heavy UHECR composition by PAO. We have also studied whether heavy nuclei could survive from photo-disintegration by

low-energy photons in the sources. In the semi-relativistic hypernova scenario, UHE nuclei can survive easily as the large size of the acceleration region leads to a low density of target photons. On the other hand, the survival probability of UHE nuclei in internal shock scenario depends on the inherent relations among the quantities of LLGRBs, such as $\varepsilon_{\gamma b}$, Γ and L . In spite of the assumptions in these relations, we find that in the luminosity range of LLGRBs that we are concerning, UHE heavy nuclei can retain most of their nucleons before escaping from the sources. Finally, the accompanying neutrino flux is calculated. The energy loss through photopion production is negligible for UHE nuclei and hence the diffuse neutrino flux from LLGRBs can hardly be detected by current detectors, except in the case of a high local rate of LLGRBs.

Our calculations indicate that local LLGRBs remain viable sources of UHECRs in terms of the energy production rate. Future GRB detectors, such as *EXIST/HET*, could cover a wider burst trigger band (5-600keV) with an advanced sensitivity of $1.5 \times 10^{-9} \text{ erg cm}^{-2} \text{ s}^{-1}$ (Imerito et al. 2008). *EXIST/HET* will increase the LLGRB detection rate by a factor of tens compared to *Swift/BAT* and *Fermi/GBM* (Imerito et al. 2008), thus much more LLGRBs could be detected. It would help us to learn more about the nature of LLGRBs and examine more carefully the connection between LLGRBs and UHECRs in future.

ACKNOWLEDGEMENTS

This work is supported by the NSFC under grants 10873009, 10973008 and 11033002, the 973 program under grants 2009CB824800 and 2007CB815404, the Program for New Century Excellent Talents in University, the Qing Lan Project and the Fok Ying Tung Education Foundation.

REFERENCES

- Abraham J., et al., 2010, *PhRvL*, 104, 091101
 Ahrens J., et al., 2004, *Aph*, 20, 507
 Allard D., Busca N. G., Decerprit G., Olinto A. V., Parizot E., 2008, *JCAP*, 10, 33
 Anchordoqui L. A., Hooper D., Sarkar S., Taylor A. M., 2008, *Aph*, 29, 1
 Band D. L., 2008, *AIPC*, 1000, 121
 Berezhinsky V., Gazizov A., Grigorieva S., 2006, *PhRvD*, 74, 043005
 Biermann P. L., Strittmatter P. A., 1987, *ApJ*, 322, 643
 Bloom J. S., Frail D. A., Sari R., 2001, *AJ*, 121, 2879
 Campana S., et al., 2006, *Natur*, 442, 1008
 Cappellaro E., Evans R., Turatto M., 1999, *A&A*, 351, 459
 Chevalier R. A., Li Z.-Y., 1999, *ApJ*, 520, L29
 Chornock R., et al., 2010, *arXiv*, arXiv:1004.2262
 Crowther P. A., 2007, *ARA&A*, 45, 177
 Dahlen T., et al., 2004, *ApJ*, 613, 189
 Dai X., 2009, *ApJ*, 697, L68
 Dermer C. D., Atayan A., 2006, *NJPh*, 8, 122
 Eichler D., Guetta D., Pohl M., 2010, *ApJ*, 722, 543
 Eichler D., 2011, *ApJ*, 730, 41
 Farrar G. R., Gruzinov A., 2009, *ApJ*, 693, 329
 Galama T. J., et al., 1998, *Natur*, 395, 670
 Garcia-Segura G., Mac Low M.-M., Langer N., 1996, *A&A*, 305, 229
 Fraternali F., Pareschi G., 2008, *MNRAS*, 390, L88
 Guetta D., Della Valle M., 2007, *ApJ*, 657, L73
 Imerito A., Coward D., Burman R., Blair D., 2008, *MNRAS*, 391, 405
 Kaneko Y., et al., 2007, *ApJ*, 654, 385
 Karakula S., Tkaczyk W., 1993, *Aph*, 1, 229
 Katz B., Budnik R., Waxman E., 2009, *JCAP*, 3, 20
 Kingsburgh R. L., Barlow M. J., Storey P. J., 1995, *A&A*, 295, 75
 Kulkarni S. R., et al., 1998, *Natur*, 395, 663
 Lemoine M., Waxman E., 2009, *JCAP*, 11, 9
 Liang E., Zhang B., Virgili F., Dai Z. G., 2007, *ApJ*, 662, 1111
 MacFadyen A. I., Woosley S. E., Heger A., 2001, *ApJ*, 550, 410
 Malesani D., et al., 2004, *ApJ*, 609, L5
 Michalowski S., Andrews D., Eickmeyer J., Gentile T., Mistry N., Talman R., Ueno K., 1977, *PhRvL*, 39, 737
 Mirabal N., et al., 2003, *ApJ*, 595, 935
 Mirabal N., Halpern J. P., An D., Thorstensen J. R., Terndrup D. M., 2006, *ApJ*, 643, L99
 Murase K., Nagataki S., 2006, *PhRvD*, 73, 063002
 Murase K., Ioka K., Nagataki S., Nakamura T., 2006, *ApJ*, 651, L5
 Murase K., Ioka K., Nagataki S., Nakamura T., 2008, *PhRvD*, 78, 023005
 Mücke A., Engel R., Rachen J. P., Protheroe R. J., Stanev T., 2000, *CoPhC*, 124, 290
 Norman C. A., Melrose D. B., Achterberg A., 1995, *ApJ*, 454, 60
 Pian E., et al., 1999, *A&AS*, 138, 463
 Pian E., et al., 2006, *Natur*, 442, 1011
 Piran T., 2010, *arXiv*, arXiv:1005.3311
 Prochaska J. X., et al., 2004, *ApJ*, 611, 200
 Puget J. L., Stecker F. W., Bredekamp J. H., 1976, *ApJ*, 205, 638
 Rachen J. P., Mészáros P., 1998, *PhRvD*, 58, 123005
 Razzaque S., Mészáros P., Waxman E., 2004, *PhRvL*, 93, 181101
 Soderberg A. M., Nakar E., Berger E., Kulkarni S. R., 2006, *ApJ*, 638, 930
 Soderberg A. M., et al., 2006, *Natur*, 442, 1014
 Sollerman J., et al., 2002, *A&A*, 386, 944
 Spiering C., 2008, *AIPC*, 1085, 18
 Starling R. L. C., et al., 2011, *MNRAS*, 411, 2792
 The Pierre AUGER Collaboration, et al., 2010, *Aph*, 34, 314
 Toma K., Ioka K., Sakamoto T., Nakamura T., 2007, *ApJ*, 659, 1420
 Vietri M., 1995, *ApJ*, 453, 883
 Virgili F. J., Liang E.-W., Zhang B., 2009, *MNRAS*, 392, 91
 von Kienlin A., et al., 2004, *SPIE*, 5488, 763
 Wang X.-Y., Razzaque S., Mészáros P., Dai Z.-G., 2007a, *PhRvD*, 76, 083009
 Wang X.-Y., Li Z., Waxman E., Mészáros P., 2007b, *ApJ*, 664, 1026
 Wang X.-Y., Razzaque S., Mészáros P., 2008, *ApJ*, 677, 432
 Wang X.-Y., Dai Z.-G., 2009, *ApJ*, 691, L67
 Waxman E., 1995, *PhRvL*, 75, 386
 Waxman E., Bahcall J., 1999, *PhRvD*, 59, 023002
 Waxman E., 2004, *ApJ*, 606, 988
 Waxman E., 2005, *PhST*, 121, 147
 Waxman E., 2010, *arXiv*, arXiv:1010.5007
 Waxman E., 2011, *arXiv*, arXiv:1101.1155

- Wick S. D., Dermer C. D., Atoyan A., 2004, *Aph*, 21, 125
Willis A. J., 1991, *IAUS*, 143, 265
Woosley S. E., Heger A., 2006, *ApJ*, 637, 914
Wu X. F., Dai Z. G., Huang Y. F., Lu T., 2003, *MNRAS*, 342, 1131
Yonetoku D., Murakami T., Nakamura T., Yamazaki R., Inoue
A. K., Ioka K., 2004, *ApJ*, 609, 935